The Study of Carrier Effects on the ESR of Vanadium Ions Formed in Supported Catalysts, as Assisted by Spectrum Calculation

Hisashi UEDA

National Chemical Laboratory for Industry, 2-19-19 Mita, Meguro-ku Tokyo 153

(Received October 17, 1978)

In order to study the carrier effects on the supported catalysts of vanadium, the ESR spectra of vanadium ions supported on γ-Al_2O_3, SiO_2, ZrO_2, TiO_2, MgO, or CaO and reduced in H_2 at 500 °C were studied. When γ-Al_2O_3, SiO_2, ZrO_2, or TiO_2 were used as the carriers, the main spectral component could be assigned to the V^{4+} ion. The results of data analysis, assisted by spectrum calculation, showed that, on catalyst which had a high activity in the reduction of NO_x by NH_3, the V^{4+} ion had a highly populated d_{xy} orbital, while on catalyst of low activity, V^{4+} had a d_{xy} with a low spin density. If the carrier was MgO, the V ion was reduced to V^{2+}. If the carrier was CaO, no ESR signals due to V ions were observed. It has been suggested that an inhomogeneous and axially symmetric crystal-field model may interpret the intensity ratios among the hyperfine lines of the V^{4+} ESR absorption rather than a non-axial symmetry model of the V^{4+} unpaired electron.

A supported catalyst of vanadium can be prepared by adsorbing vanadate ions on the surface of the carrier from an aqueous solution and then calcining them to V_2O_5. The catalyst thus prepared has catalytic activities, *e.g.*, in the reduction of nitrogen oxide by NH_3. If this catalyst is placed in a reducing atmosphere, V^{4+} is formed in some cases, depending upon the carrier used. The V^{4+} ion thus formed may participate in the catalytic reaction cycles involved. The study of the supported states of the vanadium ion and its surface concentration can be important technique for elucidating the mechanism of the reaction and the catalytic activities.

There have been many reports about the ESR spectra of V^{4+} ions, including the principal values of *g*- and hyperfine tensors (the latter to be abbreviated simply as **A** in this paper).[1-8] Most of those data were obtained from the V^{4+} ion diluted in a diamagnetic-host single crystal. A few analyses of the ESR spectra of V^{4+} porphyrin compounds, which are found in crude petroleum, have also been reported.[8] Few detailed reports about the V^{4+} ion in supported catalysts have appeared, however. The characteristic feature of the ESR spectra of the V^{4+} ion is its approximately axial symmetry and the large differences between g_z (assumed to be the rotational axis) and g_x, and between *A* and *B* (or *C*).

As the vanadium nucleus, ^{51}V, has a nuclear spin of 7/2, eight spectral lines overlap each other in the ESR spectrum of a supported vanadium catalyst in which anisotropic *g*- and *A*- tensors are averaged. In addition, the ESR absorption due to some species other than V^{4+} will also overlap the V^{4+} absorption lines in most cases. In such cases, the subtraction of the calculated V^{4+} absorption from the entire spectrum observed will yield these secondary spectral components. Spectral subtraction, therefore, is an important method in spectral analysis. First derivative curves are not, to the knowledge of the present author, convenient when the addition or subtraction of two spectra is performed. Integrated curves are more easily normalized, and with them it is more easier to grasp the meaning of the spectral components. For this reason, the absorption curve obtained by the integration of a first derivative curve will hereafter be called the "true resonance curve" in this paper.

The subtraction of spectra was performed by using true resonance curves in this work. What the first derivative curve indicates is the slope of the true resonance curve. Therefore, if more than two absorption peaks partly or fully overlap each other, the precise determination of g_z and g_x (or g_y), and *A* and *B* (or *C*) is very difficult. In these instances, the values obtained from the peak and bottom positions of the first derivative curve are nothing more than a set of crude approximation values of g_z and g_x (or g_y). In order to get more accurate results, therefore, it is advisable to repeat the spectral simulation procedures.

In order to analyse the ESR spectra of the V^{4+} ion formed on the surface of γ-alumina powder, the spectral simulation method should be very useful for the reason stated above. However, only a little work has been done on this subject, using the type of samples described above. Campadelli and Bart analysed the line shape of the $MoO_3 \cdot Al_2O_3$ catalyst considering the *g*-value dispersion and the spin-spin interaction. Their calculation did not cover the entire region in which the experimental spectra had absorption intensities. It is not clear, therefore, if their assumption that the line width was caused only by the *g*-value dispersion and by spin-spin interactions was correct or not.[9]

Experimental, Data Processing, and Simulation

Preparation of ESR Samples. The oxides used as carriers of V_2O_5 were γ-alumina (Baikowski, A125-AS2, 148 m^2/g), silica gel (Fuji Davison, SP-No. 3, 153 cm^2/g), zirconium oxide (Mitsuwa Chemical Co., 99.9% pure, 8.5 m^2/g), titanium oxide (Kokusan Chemical Co., 7.4 m^2/g), magnesium oxide (Nihon Rikagaku, Inc., 89 m^2/g), and calcium oxide (Junsei Pure Chemicals, 3.0 m^2/g, containing alkali metals and magnesium as impurities, the sum being less than 2%). These oxides were mixed with an aqueous solution of ammonium vanadate from which mixture water was evaporated at room temperature. After drying at 100 °C, they were calcined at 550 °C in air to form V_2O_5. The final concentration in the solid mixtures obtained was 0.5%. The solid sample was then placed in a quartz tube 8 mm in inner diameter and was reduced at 500 °C with H_2 at 1 atm pressure and at the flowing rate of 50 ml/min for 1 h. Some of the V^{4+} ions contained in this sample were reduced to

some extent. The sample was cooled in the hydrogen atmosphere and was then taken out into the air. It was then placed in a ESR sample tube and ESR measurements were made while evacuating it to 10^{-5} Torr.

The results obtained are shown in Figs. 1—9, together with the simulated spectra. For the purpose of comparison, a sample of $VOSO_4$ supported on γ-alumina was prepared. In this case, 1.0 mg of $VOSO_4 \cdot 2H_2O$ was mixed with 5.0 ml of redistilled water and 1 g of γ-alumina. After the water has been evaporated, it was vacuum-dried and then used for ESR measurements. Although the official SI unit representation of the magnetic-field flux density is Tesla, T, a conventional symbol, G, is used in this report to represent 0.0001 T.

Data Processing. The output of an ESR spectrum from the spectrometer is in the form of DC voltage from 0 to 10 mV. This voltage is converted to natural numbers at the rate of 10 mV to 256. The numbers are stored in JEC-5 computer of JEOL and are then punched out on paper data tape. This spectrum is then integrated by a Fortran system of Hitac 10 II.

Spectrum Simulation. Several types of programming methods have been established to calculate the ESR spectra of the paramagnetic species existing in polycrystalline or multioriented substances.[10-13] These methods, however, have been contrived to be executed by large computers. Therefore, if one intends to handle the calculation problem simply as a matter of calculation, those past works will assist the researcher to a great extent. However, if one is intending to use the calculation as a part of his experimental system, it often happens that one cannot afford to use a large computer in his experimental system. In the present work, a calculation method which is essentially the same as those in the past reports, but which is modified so as to make it suitable for the computing system used in the present study, has been used.

The calculation was done by the Fortran system described above, and the result was displayed on a conventional paper chart recorder placed after a digital-analogue converter.[14] In the present problem, the spin Hamiltonian can be written:

$$\mathscr{H} = (g_z S_z + g_x S_x + g_y S_y)\beta H + (AS_z + BS_x + CS_y)I.$$

According to this equation, the calculation of the spectra may be carried out in three different ways. In the first case, $g_z \neq g_x \neq g_y$ and $A \neq B \neq C$. In the second case $g_z \neq g_x = g_y$ and $A \neq B = C$. In the third case $g_z = g_x = g_y$ and $A = B = C$. The third case does not have to be considered in the present work. The g-factor and coupling constant, *e.g.*, A, were surveyed in the $g \pm 0.001$ and $A \pm 0.0002$ regions, and the best combination was judged by a visual inspection.

Results

In Figs. 1—7 the spectra obtained by both experiments and calculations are shown. The true absorption of ESR is plotted, except in Fig. 1, with the magnetic field increasing from right to left. The parameters used for the calculations is shown in Table 1. The first derivative curve of the spectrum of Fig. 2 is shown in Fig. 1. The sample which gave these spectra was V_2O_5/TiO_2 reduced in H_2. The "OBS" in Fig. 1 means the observed spectrum, while "SIM" means that obtained by spectral simulation. The vertical lines shown in the figures indicate the positions of resonance, with $(h\nu/g_z\beta)+m_I A$ shown by longer lines and $(h\nu/g_x\beta)+m_I B$ shown by shorter lines, in which A and B are in the unit of the magnetic field, G. An axial symmetry is assumed, $B=C$. The z-direction is taken as the symmetry axis.

TABLE 1. THE ESR CONSTANTS FOUND BY SPECTRAL SIMULATION

Carrier	Ion	g_z	g_x, g_y	A/cm^{-1}	B/cm^{-1}	Half-width/T[a]
TiO_2	V^{4+}	1.9400	1.9892	0.0160	0.0050	0.00632
ZrO_2	V^{4+}	1.9036	1·9735	0.0170	0.0070	0.00200
SiO_2	V^{4+}	1.9333	1.9807	0.0102	0.0048	0.00365
Al_2O_3	V^{4+}	1.9494	1.9828	0.0165	0.0055	0.00632
Al_2O_3	VO^{2+}	1.9490	1.9980	0.0174	0.0067	0.00316

a) Simulation by Lorentz function.

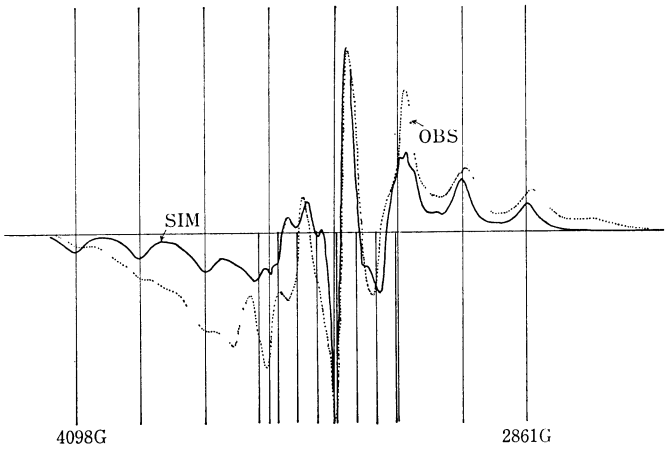

Fig. 1. The first derivative curve of ESR spectrum of hydrogen reduced 0.5% V_2O_5/TiO_2 sample. Microwave power was 0.4 mW, and at 9450 MHz. Vertical lines indicate the positions of the principal values, Table 1.

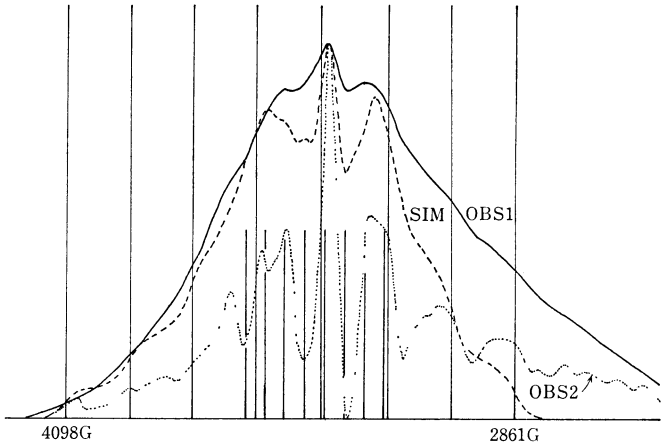

Fig. 2. True absortion curves of the spectra in Fig. 1.

The peak and the bottom positions in the outer part of the spectrum in Fig. 1 almost exactly coincide with the magnetic-field value given by the principal values of $\boldsymbol{g}$ and $\boldsymbol{A}$. Therefore, g and A may be found by solving this equation: $H=(h\nu-Am_I)/g_z\beta$ using a first derivative curve. However, the magnetic-field values for the $H=(h\nu-Bm_I)/g_x\beta$ equation are extremely difficult to find because the central part of the spectrum

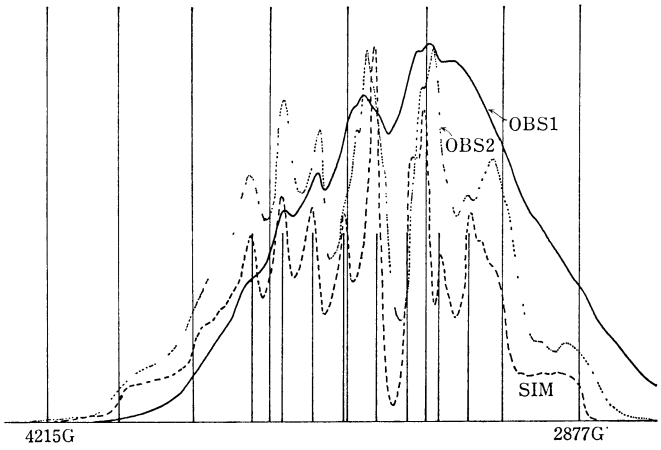

Fig. 3. 0.5% V_2O_5/ZrO_2. Other conditions identical with those of Fig. 2.

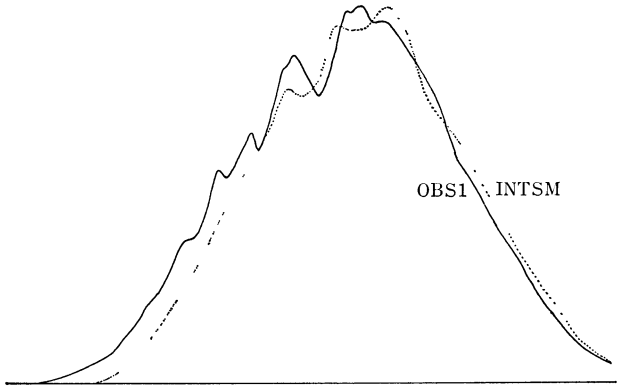

Fig. 4. Sample used was the same as that for Fig. 3.

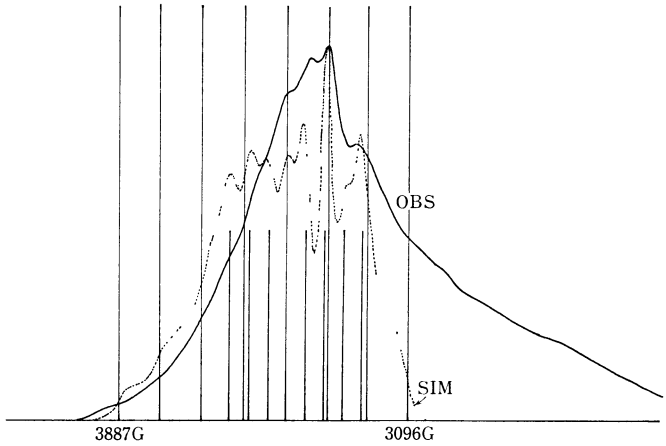

Fig. 5. 0.5% V_2O_5/SiO_2. Other conditions identical with those of Fig. 2.

is crowded overlapping spectral lines. In these cases, Kneubühl's equation is very hard to apply.[15]

In Fig. 2, OBSl is the observed spectrum. OBSSM was obtained from OBSl by the following processing method. At every magnetic-field point of the OBSl spectrum, the absorption intensities were integrated over the ±40 G region and were then averaged, the average being registered as the intensity of OBSSM at that field value. From this smoothed curve, OBS2′= OBS1−OBSSM was calculated. By the normalization

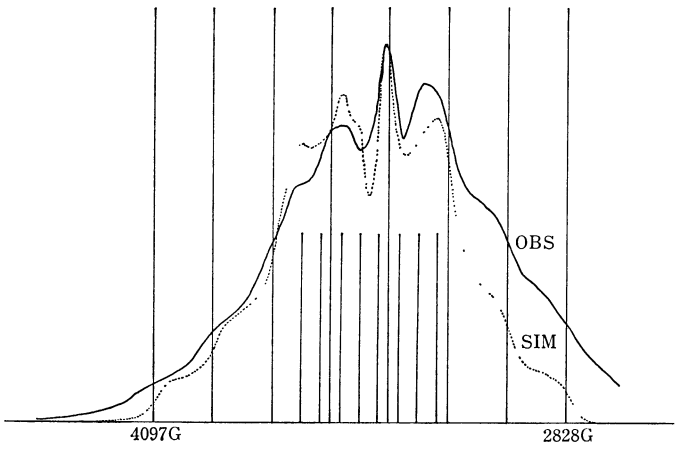

Fig. 6. 0.5% V_2O_5/γ-Al_2O_3. Other conditions are identical with those of Fig. 2.

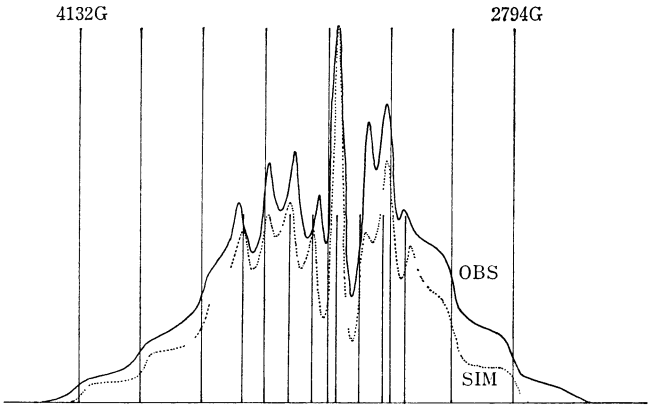

Fig. 7. 1.0 mg of $VOSO_4 \cdot 2H_2O$ dispersed on the surface of 1.0 g of γ-Al_2O_3.

of OBS2′, OBS2 was obtained. The hyperfine structures are found more clearly in OBS2, which makes the estimation of B and g easier.

The V^{4+} spectra formed in reduced V_2O_5/ZrO_2 are shown in Fig. 3. The observed spectrum is OBS1. The explanation for OBS2 will be made later. The SIM spectrum was obtained by calculations using the parameters found in OBS1. The OBS1 spectrum contains two component spectra. One of them has the hyperfine structure of the OBS2 of Fig. 2, or the normal V^{4+} hyperfine structure. The other component has a somewhat different structure. The INT spectrum, which is not shown in the figure, was made from OBS1 and SIM; INT=OBS−0.352 SIM. The INTSM spectrum was obtained by smoothing the INT spectrum in the same way as was used to get the OBS2 of Fig. 2. INTSM is shown in Fig. 4 with OBS1.

A hyperfine structure different from that of OBS1 is found in INTSM, but it was not analysed. The OBS2 spectrum of Fig. 3 was obtained as OBS1−0.813 INTSM. The parameters found in OBS2 were compared with those obtained from OBS1. Since there was some difference between these two groups of parameters, the SIM spectrum was again calculated from the data found in OBS2. By repeating the procedure described above, the INT, the INTSM, and the OBS2 spectra were again calculated. The

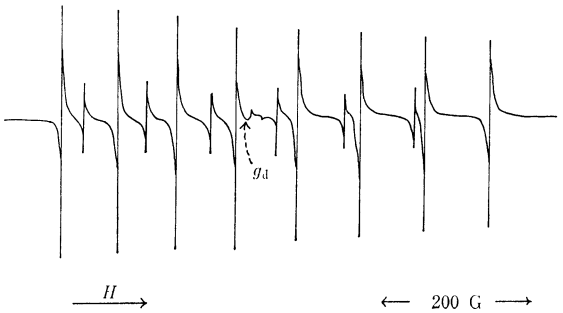

Fig. 8. 0.5% V_2O_5/MgO. Other conditions are identical with those of Fig. 3.

final agreement of OBS2 with SIM was fairly good.

The ESR spectrum of the V^{4+} ion formed in reduced V_2O_5 supported on SiO_2, OBS, and the spectrum calculated to fit it, SIM, are shown in Fig. 5. The silica gel used has some impurities. The intensity of the absorption by V^{4+} in this sample is not strong. For these two reasons, the background ESR spectrum, BG, which is not shown, was subtracted from the originally observed spectrum, OROBS, which is not shown, either. Therefore, OBS=OROBS−BG. A broad component, V, is found in the OBS spectrum in addition to the spectrum with the V^{4+} hyperfine structure. This circumstance is similar to those shown in Figs. 3 and 4.

The ESR spectra of the V^{4+} ion formed in the reduced V_2O_5 on γ-alumina are shown in Fig. 6. Since the carrier used in this sample was very pure and gave no appreciable absorption, and since the ESR absorption of V^{4+} on γ-alumina was relatively strong, the OBS spectrum itself could be fitted well by the calculated spectrum. The ESR spectrum of the VO^{2+} ion which was adsorbed on γ-alumina and the spectrum calculated to fit it are shown in Fig. 7. In Fig. 6 the half-width used for the calculation was 63.2 G, but in Fig. 7 31.6 G gave a good fit. Here the difference between VO^{2+} and V^{4+} is quite clear. No ESR spectra which are like those in Figs. 1—7 could be observed from the sample in which the carrier oxide was either CaO or MgO. If the carrier was CaO, no ESR signal due to V ions were observed. In the case of MgO, the spectrum shown in Fig. 8 was observed. It is not V^{4+} but V^{2+} that gives this spectrum.[16] The position of the magnetic field indicating $g=2.0036$ is marked by an arrow and g_d. The results obtained by CaO and MgO indicate that, on the surface of these alkaline earth oxides, V^{4+} is not stable.

Discussion

The Electronic State of the d-Electron and the Carrier Effects on It. The hyperfine splitting values observed from the V^{4+} ion have two components, the isotropic term and the anisotropic term. For the electron in a d^1 configuration, either the d_{z^2} or d_{xy} orbital is concluded to hold the unpaired electron.[5] The molecular orbital formed between the ligand orbital, $\psi_L(xy)$, and d_{xy} is denoted by π. Let β and β' be the proper coefficients, then:

$$\pi = \beta d_{xy} - \beta'\psi_L(xy).$$

Table 2. The K and β^2 values

Carrier	Ion	K/cm^{-1}	β^2
SiO_2	V^{4+}	0.0242	0.375
Al_2O_3	VO^{2+}	0.0229	0.727
ZrO_2	V^{4+}	0.0222	0.690
Al_2O_3	V^{4+}	0.0206	0.754
TiO_2	V^{4+}	0.0200	0.751

The β in this equation is different from that used in the spin Hamiltonian. The spin Hamiltonian is, if all the spectra are approximated by axially symmetric models:

$$\mathscr{H} = g_z\beta H_z S_z + g_x\beta[H_x S_x + H_y S_y] + AI_z S_z + B[I_x S_x + I_y S_y].$$

From the ESR spectrum, the hyperfine coupling constants, A and B, are obtained. A and B are shown by the following equations:[17–19]

$$A = -K - (4/7)\beta^2 P + (g-2.0023)P + (3/7)(g-2.0023)P$$

$$B = -K + (2/7)\beta^2 P + (11/14)(g-2.0023)$$

The value of P is equal to $2.0023 \cdot g_N \cdot \beta \cdot \beta_N \cdot \langle r^{-3} \rangle$, and the value for $^{51}V^{4+}$ is 0.0172 cm^{-1}.[20] Therefore, K and β^2 are solved from the above equations. Those values calculated from the data in Table 1 are shown in Table 2.

The isotropic contact term in the hyperfine interaction of paramagnetic ions has been the subject of many studies.[20–22] Abragam, Horowitz, and Pryce have observed that the quantity, χ, defined as:

$$\chi = \frac{4\pi}{S}(\psi | \sum \delta(r_i) S_{zi} | \psi)$$

is negative and nearly constant in magnitude for ions in the first transition series.[21] The χ value is related with K by means of the following equation:[21]

$$\chi = \left[-\frac{3}{2}\left(\frac{hca_0^3}{2.0023\, g_N \beta \beta_N} \right) K \right].$$

In this equation, h is Planck's constant, c is the velocity of light, a_0 is the Bohr radius, and g_N is 5.050 for ^{51}V. Therefore, the K value is proportional to the probabilities of the 2s and 3s electrons to be excited to the 3d orbital. In Table 2, the K value for V^{4+}/SiO_2 is the largest and the one for V^{4+}/TiO_2 is the smallest. The β^2 value is proportional to the spin density in d_{xy}, and the values are in a decreasing order when the samples are V^{4+}/Al_2O_3, V^{4+}/TiO_2, V^{4+}/ZrO_2, and V^{4+}/SiO_2.

The catalytic activity of V_2O_5 supported on TiO_2, ZrO_2, SiO_2, and Al_2O_3 greatly depends upon the carriers. It has been considered that the specific surface areas of these carriers are different. The TiO_2 used has only 7.4 m^2/g, while the SiO_2 used had 153 m^2/g. There are several types of reactions in which γ-alumina works as a good carrier. If used as a carrier of the supported catalyst applied to these types of reactions, the carrier effects of those oxides decrease in this order: γ-alumina, ZrO_2, TiO_2, and SiO_2. From the values of K and β^2 shown in Table 2, it may be concluded that the highly active V^{4+} ion has a d_{xy}

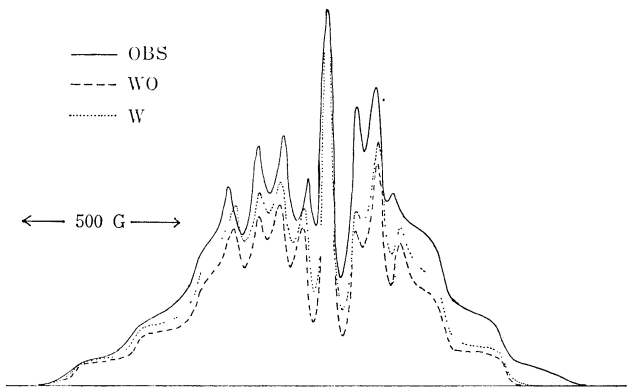

Fig. 9. True absorption curves showing the effect of axial distortion on the ESR spectrum. WO: Spectrum for the ion without axial symmetry. About parameters, see text. W: Spectrum identical with Fig. 7-SIM. OBS: Identical with Fig. 7-OBS.

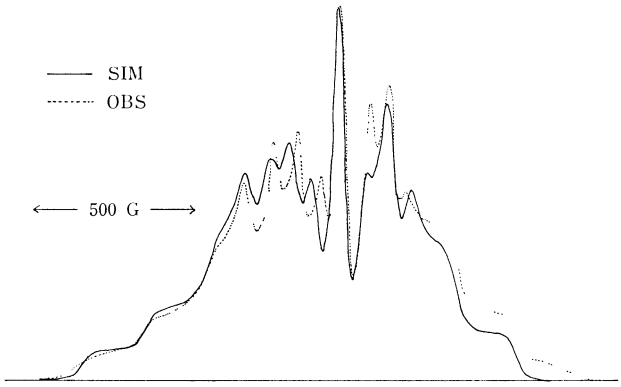

Fig. 10. True absorption curves demonstrating the effect of inhomogeneous crystal fields on the ESR spectrum. SIM: An equal mixture of two spectra, parameters are in text. OBS: Identical with Fig. 7-OBS.

orbital which extends well toward the x and y directions, as an ideal d_{xy} orbital should, or that d_{xy} has a high spin density.

Axial Distortion or Inhomogeneous Crystal Field. Broad spectral components are found in Figs. 2—5 in addition to the hyperfine spectral components. Some of them are due to some impurities in the carrier. However, many of the broad components are caused by the minor distortions and the irregular crystal fields. The V^{4+} ions on the surfaces of TiO_2, ZrO_2, and SiO_2 particles may be surrounded by these partially distorted crystal fields. Another minor irregularities of the crystal field can also be expected from the half-width value of 63 G used in the calculation of the spectrum (Table 1). Sixty-three gauss, if it is caused by the irregular g-tensor, is equivalent to $\delta g=0.036$. Therefore, if we assume a mixture of two V^{4+} ions placed in two different environments which cause the principal values of the g-tensor to differ by some 0.036, the 63 G half-width can be explained.

The approximation of the calculated spectrum SIM in Fig. 7 is not satisfactory if the intensities of the absorption peaks are considered. The first thing to be examined is if the axial symmetry assumed in this work is effective or not. Figure 9 compares two spectra with and without axial symmetry. The WO spectrum was derived by the use of $g_z=1.9490$, $g_x=1.9955$, $g_y=2.0005$, $A=0.0174$, $B=0.0068$, $C=0.0066$ cm^{-1}, and a half-width of 23.62 G. The intensity ratios, especially that of the strongest peak to those of the remaining peaks, rather deviate from that of the OBS spectrum. Therefore, it does not seem possible to interpret the large line-width in terms of the axial distortion only. Among other factors to be considered is the inhomogeneity of the crystal field surrounding the V^{4+} ions, which might be located on the edge, on the ridge, or in the valley or the deep holes existing on the surface of the carrier particles. Figure 10 shows one attempt to study this subject. The OBS spectrum is identical with the one in Figs. 7 and 9. The SIM spectrum was derived from the two spectra as an arithmetic mean. The one of the component spectra was the Fig. 7-SIM spectrum. The other component spectrum was calculated by means of $g_z=1.9599$, $g_x=g_y=2.0092$, $A=0.00174$, $B=C=0.0067$ cm^{-1}, and a half-width of 31.62 G. The agreement of the intensity ratios have been fairly well improved.

The large line-width of the paramagnetic ions located on the surface of porous powders includes many factors which it is not easy to solve or to understand fully. In the case of a nucleus which has a large nuclear spin, such as V^{4+}, the spin Hamiltonian has a nuclear quadrupole term, *e.g.*, $Q'(I_z^2-63/12)$. If the axis of the magnetization is perpendicular to the z-axis, secondary transitions can occur between energy levels; therefore, the experimental ESR spectrum may not be accounted for by simply averaging the ESR spectra which are obtained from the V^{4+} ions oriented in random directions in the magnetic field. The strongest absorption peak of the OBS spectrum in Fig. 7 is relatively weaker than that which is to be expected by the calculated spectrum, SIM. This fact might be explained if one would consider the nuclear quadrupole term. However, it seems to the present author that the angular variation of the intensity ratio of the hyperfine lines should be studied by means of a system which is simpler than the supported catalysts used in this work. For this reason, such considerations have not been undertaken here. At any rate, the inhomogeneous crystal-field approach will solve a part of this problem.

CaO and MgO as Carriers. When used as the carrier of a catalyst for a reaction in which γ-alumina works as a good carrier of the catalyst, CaO and MgO are poor carriers. It seems there are no such sites as keep the V^{4+} ion stable on the surfaces of these oxides. In the case of MgO, a Mg^{2+} vacancy will be replaced by a V^{4+} ion, which is then reduced to the $+2$ oxidation state if placed in a H_2 atmosphere above 500 °C. The V^{2+} ion thus formed is stable, probably because it is somehow equivalent to Mg^{2+} with respect to the electrostatic field that is produced in the surrounding crystal lattice.

References

1) F. W. Lancaster and W. Gordy, *J. Chem. Phys.*, **19**, 1181 (1952).

2) C. A. Hutchison and L. S. Singer, *Phys. Rev.*, **89**, 256 (1953).
3) K. D. Bowers and J. Owen, *Rep. Prog. Phys.*, **18**, 96 (1958).
4) C. J. Ballhausen, "Introduction to Ligand Field Theory," McGraw-Hill Book Co., New York, N. Y. (1962), p. 228.
5) C. J. Ballhausen and H. B. Gray, *Inorg. Chem.*, **1**, 111 (1962).
6) P. W. Lau and W. C. Lin, *J. Chem. Phys.*, **59**, 3998 (1973).
7) M. Marayana, S. G. Sathanaryan, and G. S. Sastry, *Mol. Phys.*, **31**, 203 (1976).
8) D. E. O'Reilly, *J. Chem. Phys.*, **29**, 1188 (1958).
9) F. Campadelli and J. C. Bart, *React. Kinet. Catal. Lett.*, **3**, 435 (1975).
10) A. C. Ling, *J. Chem. Educ.*, **51**, 174 (1974).
11) H. A. Buckmaster, R. Chatterjee, J. C. Dering, D. J. Fry, Y. H. Shing, J. D. Skirrow, and B. Venkatesan, *J. Magn. Reson.*, **4**, 113 (1971).
12) R. Lefebvre and J. Maruani, *J. Chem. Phys.*, **42**, 1480 (1965).
13) K. Kuwata, "Kagaku To Denshikeisanki," ed by T. Yonezawa and K. Osaki, Nankodo, Tokyo, Japan (1968), p. 95.
14) H. Ueda, *Bull. Chem. Soc. Jpn.*, **49**, 2343 (1976); *J. Catal.*, **47**, 284 (1976).
15) F. K. Knebühl, *J. Chem. Phys.*, **33**, 1074 (1960).
16) W. Low, *Phys. Rev.*, **101**, 1827 (1956).
17) D. Kivelson and R. Neiman, *J. Chem. Phys.*, **35**, 149 (1961).
18) H. R. Grasman and J. D. Swallen, *J. Chem. Phys.*, **36**, 3221 (1967).
19) A. H. Maki and B. R. McGarvey, *J. Chem. Phys.*, **29**, 31, 35 (1958).
20) B. R. McGarvey, *J. Phys. Chem.*, **71**, 51 (1967).
21) A. Abragam, J. Horowitz, and M. H. L. Pryce, *Proc. R. Soc. London, Ser. A*, **230**, 169 (1955).
22) A. J. Freeman and R. E. Watson, "Magnetism," ed by G. T. Rado and H. Suhl, Academic Press, New York, N. Y. (1965), Vol. IIA, p. 167.